

Spectral properties of chiral carbon nanoparticles based on glutathione

© E.A. Stepanidenko¹, M.D. Miruschenko¹, A.V. Koroleva², E.V. Zhizhin², A.M. Mitroshin^{1,3},
P.S. Parfenov¹, S.A. Cherevko^{1,*}, E.V. Ushakova¹

¹ International research and educational center for physics of nanostructures, ITMO University,
197101 Saint-Petersburg, Russia

² Research Park, Saint Petersburg State University,
199034 Saint-Petersburg, Russia

³ Institute of Macromolecular Compounds, Russian Academy of Sciences,
199004 Saint-Petersburg, Russia

e-mail: s.cherevko@itmo.ru

Received December 06, 2023

Revised December 06, 2023

Accepted December 11, 2023

In this work, carbon nanoparticles (C-dots) were obtained from solution of chiral L-glutathione molecules in formamide. The resulting C-dots have photoluminescence (PL) in the red region of the spectrum at 370–470 nm and a high quantum yield for this band, reaching 10.8%. In the circular dichroism spectra of these C-dots, a signal in the optical transition region of 370–470 nm, associated with sp^2 -hybridized carbon domains doped with nitrogen and oxygen atoms was observed.

Keywords: carbon dots, red photoluminescence, circular dichroism, chirality, glutathione.

DOI: 10.61011/EOS.2023.12.58185.5833-23

Introduction

In the last decade, luminescent carbon nanoparticles (C-dots) have attracted increasing attention due to their unique properties, such as low toxicity, high photoluminescence (PL) quantum yield (QY) values, and the possibility of tuning the position of optical transitions throughout the entire visible spectrum [1]. The simplicity and low cost of synthesis and the possibility of production of stable colloidal solutions in various media make C-dots attractive for use as active materials in optoelectronics [2,3], photovoltaics [4], sensorics [5], catalytic systems [6], and biomedical applications [7,8]. In biomedicine (specifically, bioimaging), nanoparticles with optical transitions in the regions of tissue transparency (red and near-infrared (NIR) spectral regions) [9] are of particular interest. Methods for synthesis of C-dots with transitions in the spectral ranges of interest involving organic dyes [10], mixtures of citric acid and urea in dimethylformamide [11,12], citric acid in formamide [13,14], etc., have been developed. Another important parameter of the interaction of nanoparticles with biological objects is chirality [15,16]. The methods for preparation of chiral C-dots can be divided into two classes: one-step approaches, where chiral molecules are used as precursors in solvothermal or microwave heating [17], and two-step ones, where chiral molecules are covalently attached to the surface of C-dots as a result of their chemical treatment in solution [18].

Taking the above into account, the most attractive objects for biological applications are C-dots that feature both optical transitions in the red/NIR region of the spectrum

and a chiral surface for controlled interaction with biological objects. Glutathione (an organic molecule with chiral groups) is one of the most suitable precursors for such nanoparticles. It has been shown that heating glutathione in a formamide solution in an autoclave leads to the formation of C-dots with a photoluminescence band positioned in the 650–710 nm region [19,20]. However, the chiral properties of such C-dots have not been studied yet. The aim of this work was to investigate the spectral characteristics of C-dots obtained solvothermally from glutathione in formamide. These 4-nm-sized nanoparticles exhibit bright photoluminescence with a band maximum at 690 nm and a circular dichroism signal in the 370–470 nm region, where the optical transition of the C-dot core is located.

Materials and research methods

Materials

Formamide ($\geq 99.0\%$), L-glutathione ($\geq 98.5\%$), and polyethylene glycol (molecular weight 2000, PEG-2000) were used in this work. All chemical reagents were used without further purification. Deionized (DI) water (Milli-Q water) was used in experiments.

Synthesis of carbon nanoparticles

C-dots were synthesized by a one-step solvothermal method from L-glutathione (94 mg) in formamide (10 mL) in a closed stainless steel autoclave at 160°C within 6 h. After the reaction, the mixture was cooled to room temperature naturally and dialyzed in DI water using dialysis bags

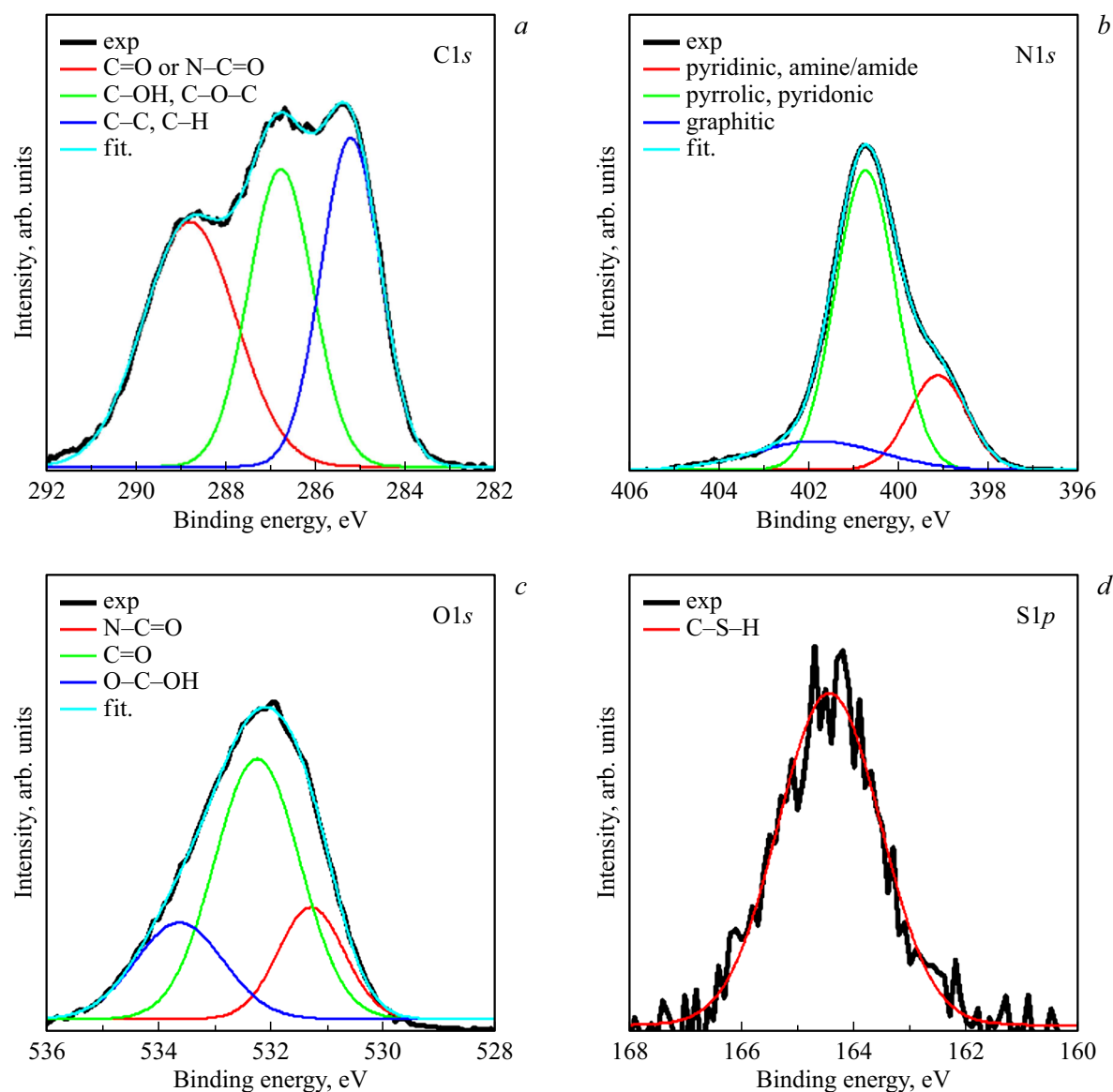


Figure 1. High-resolution XPS spectra of the CD-Glu-Ref sample: (a) C1s, (b) N1s, (c) O1s, and (d) S2p. Experimental (exp., black lines) and approximation (fit, colored lines) data with characteristic bands of different chemical groups indicated.

with a molecular weight cut-off (MWCO) of 3.5 kDa for 4 days. The sample was filtered using a syringe filter with a pore size of $0.22\ \mu\text{m}$ and lyophilized. A green powder of CD-Glu-Ref C-dots was obtained as a result.

To obtain C-dots with more stable properties, it is common to add polymer to the reaction mixture during synthesis. In order to verify this statement, an additional 13 mg of PEG-2000 were added to the basic precursors. Further synthesis was carried out similarly to the previous sample. The obtained C-dots are designated as CD-Glu-PEG below.

Research methods

The sample sizes were analyzed by atomic force microscopy (AFM) with a Solver PRO-M microscope (NT-

MDT, Moscow, Russia) in the semi-contact mode. Infrared (IR) spectra were measured with a Tensor II spectrophotometer (Bruker, Billerica, USA). X-ray photoelectron spectroscopy (XPS) was used for elemental analysis of the obtained nanoparticles. Spectra were measured using an ESCALAB 250Xi photoelectron spectrometer (Thermo Fisher Scientific, Waltham, USA) ($\text{AlK}\alpha$ radiation, the photon energy was 1486.6 eV). Absorption spectra of the solutions were obtained using a UV-3600 spectrophotometer (Shimadzu, Kyoto, Japan); maps of the photoluminescence (PL) intensity distribution as a function of sample excitation wavelength (PL-PL maps) were recorded with a Cary Eclipse spectrofluorimeter (Agilent, Santa Clara, USA). Circular dichroism (CD) absorption spectra were recorded by a J-1500 spectrophotometer (Jasco, Tokyo, Japan).

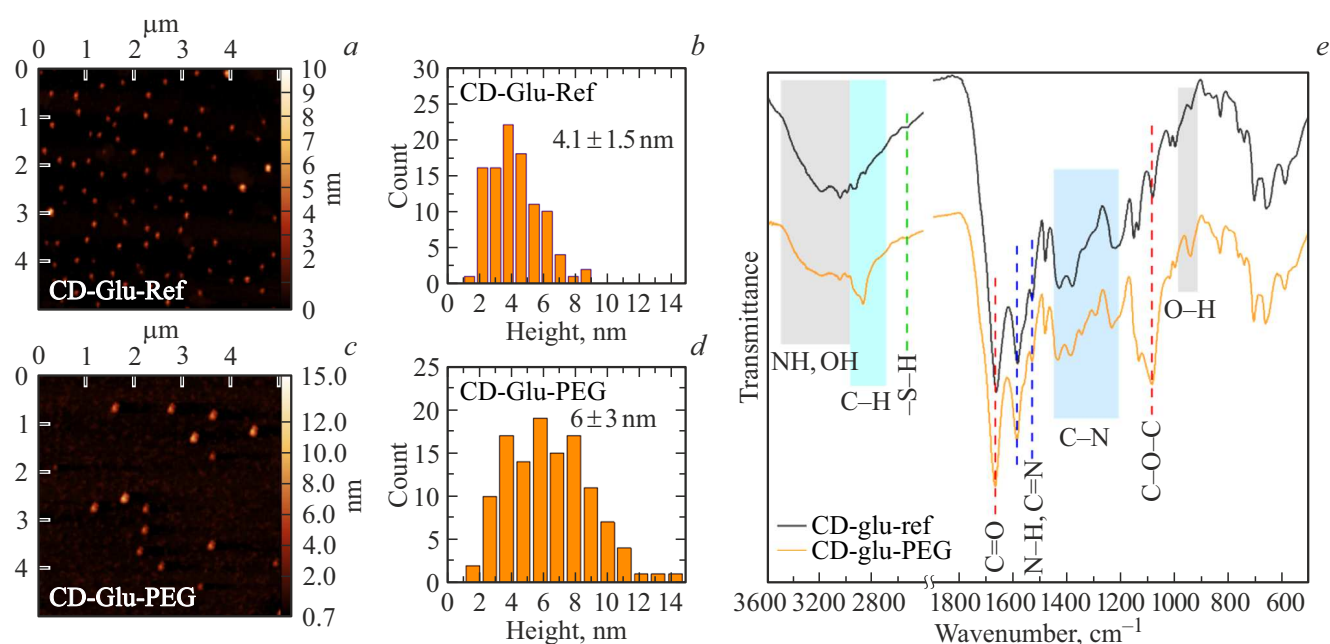


Figure 2. AFM images (*a, c*) and corresponding height distributions (*b, d*) of the CD-Glu-Ref (*a, b*) and CD-Glu-PEG (*c, d*) samples. IR spectra of samples with marked areas typical of the vibrations of different bonds (*e*).

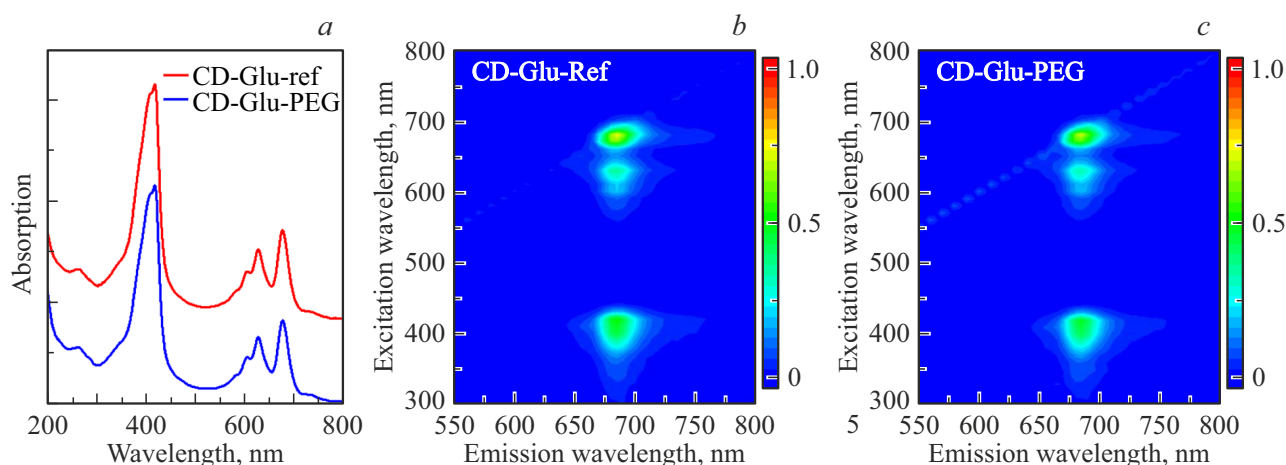


Figure 3. (*a*) Absorption spectra and (*b, c*) PL-PLE maps of aqueous solutions of CD-Glu-Ref (*b*) and CD-Glu-PEG (*c*).

Results and discussion

XPS spectra were recorded to investigate the chemical structure of C-dots based on glutathione and formamide. The panoramic XPS spectrum revealed that CD-Glu-Ref is composed of the following major elements: carbon (C1s, 55.28%), oxygen (O1s, 24.97%), nitrogen (N1s, 19.61%), and a small amount of sulfur (S2p, 0.14%). High-resolution spectra for the C1s, N1s, O1s, and S2p bands and their decomposition into peaks corresponding to different bonds are shown in Fig. 1. Based on the analysis of the C1s band, the presence of bonds C–C/C–H (285.2 eV), C–OH/C–O–C (286.7 eV), and C–N/R–C=O (288.8 eV) (Fig. 1, *a*) was established. C-dots contain a large amount of nitrogen

(19.61%), primarily in the forms of pyrrole/pyridone (400.7 eV), pyridine, and in the composition of amides and amines (399.1 eV). The sample also contains a small amount of graphite-like carbon nitride (401.8 eV) (Fig. 1, *b*). The XPS spectrum for the O1s band shows that C=O bonds prevail in the composition of amides and carboxylic groups (peaks at 531.3, 532.2, and 533.6 eV Fig. 1, *c*). A small amount of sulfur in the form of thiol (164.4 eV, Fig. 1, *d*) was also found in the sample.

Figure 2, *a–d* shows typical AFM images and the corresponding particle height distribution diagrams. The average height of CD-Glu-Ref particles was estimated at 4.1–1.5 nm (Fig. 2, *a, b*). When polyethylene glycol was added to the reaction mixture, larger nanoparticles

Quantum PL yield of aqueous solutions of C-dots

Sample	Quantum yield, %	
	$\lambda_{\text{ex}} = 400 \text{ nm}$	$\lambda_{\text{ex}} = 620 \text{ nm}$
CD-Glu-Ref	9.5	10.8
CD-Glu-PEG	8.4	10.2

formed. Specifically, a broad distribution with an average value of $6 \pm 3 \text{ nm}$ was observed for CD-Glu-PEG, and aggregates up to 15 nm in size were present in the sample (Figs. 2, c, d). The analysis of IR spectra showed that the addition of polymer in the synthesis practically does not affect the formation of bonds in C-dots: all characteristic bands in the IR spectra are repeated for both samples (Fig. 2, e). A small number of S–H= bonds were detected, as indicated by the peak at 2535 cm^{-1} . The broad absorption band at $3000\text{--}3400 \text{ cm}^{-1}$ corresponds to H-bond vibrations, and the peaks at 3200 cm^{-1} correspond to N–H valence vibrations. The peaks at 2848 and 2930 cm^{-1} represent the C–H bonds of aliphatic groups, and they are more intense in the CD-Glu-PEG sample, indicating the presence of a polymeric aliphatic chain. The peaks at 1346 and 3040 cm^{-1} correspond to valence vibrations of C–N and C–H bonds in the aromatic ring. The peaks at 1295 , 1230 , and 1085 cm^{-1} may indicate the presence of (NH)–C=O groups and C–O vibrations within C-dots, respectively. Narrow intense peaks at 1667 , 1590 , and 1530 cm^{-1} correspond to valence vibrations C=O and deformation vibrations of N–H in amides. In addition, C=C vibrations of aromatic rings may be present in this region ($1660\text{--}1550 \text{ cm}^{-1}$). The absorption around 1150 and 1134 cm^{-1} can be explained by C–O–CC vibrations, and the peak at 1150 cm^{-1} can be related to the deformation vibrations of N–H in (NH₂)–C=O. Consequently, aromatic domains doped with nitrogen and oxygen are present in the samples, and there is a multitude of amino groups on the surface of C-dots, which correlates with the XPS results. A significant number of aliphatic carbon groups are observed in the CD-Glu-PEG sample due to the presence of polymer, which also correlates with the AFM results and explains the larger size of CD-Glu-PEG compared to CD-Glu-Ref.

Analysis of the spectral characteristics of the samples showed that the addition of polymer does not lead to the formation of new optical centers, as can be seen from Fig. 3. In the absorption spectrum of both samples, a weakly intense peak at 260 nm is observed, which can be attributed to the presence of benzene and its derivatives (Fig. 3, a). The most intense absorption peak is observed at $405\text{--}417 \text{ nm}$, and the vibrational structure is pronounced in the long-wavelength band with peaks at 578 , 603 , 627 , 675 , and 734 nm . Optical transitions in the $400\text{--}415 \text{ nm}$ and $600\text{--}690 \text{ nm}$ regions represent the long-wavelength PL band with a maximum at 690 nm (Fig. 3, b, c). The PL QY was $8\text{--}11\%$, its value depending on excitation wavelength

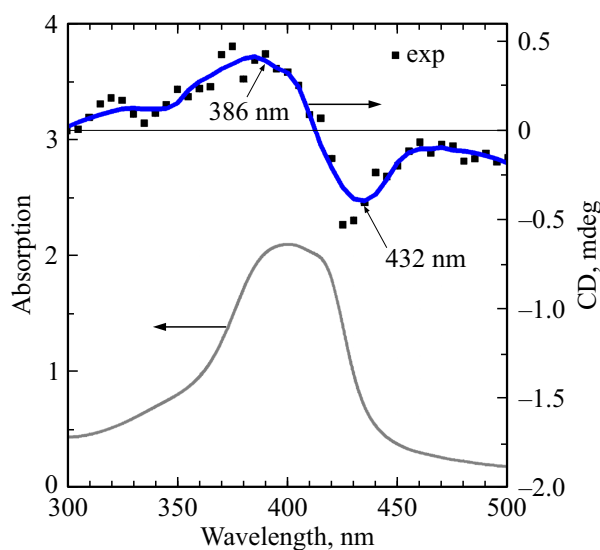


Figure 4. Absorption spectrum (gray line) and averaged circular dichroism signal (black squares and blue line) for the CD-Glu-Ref sample in water.

λ_{ex} and the sample (see the table). As expected, the use of polymer during synthesis enhances the PL QY; however, as can be seen from the table, the PL intensity of the unmodified sample is slightly higher, indicating that in this case PEG-2000 does not interact with the PL centers of C-dots.

The analysis of literature data showed that the PL band of glutathione-based C-dots almost always has a maximum at 690 nm and is independent of the excitation wavelength, which is typical of organic luminophores. Y. Ganjkanlou et al. [21] showed that this PL band has a similar nature to the Q-band emission of macromolecules — derivatives of porphyrin. The authors of this work demonstrated that macromolecules form amorphous aggregates when drying on substrates. In our experiments, no large aggregates were observed; rather, the nanoparticle height distribution in both samples did not exceed 10 nm . Having performed thin-layer chromatography, we did not detect separation of the sample into several nanoparticle fractions. Therefore, the synthesis process forms a single type of C-dots. Thus, it can be assumed that the observed long-wavelength PL is caused by optically active centers similar to porphyrin derivatives embedded in an amorphous carbon matrix of C-dots.

Since L-glutathione is a chiral molecule, we assumed that as a result of synthesis, either entirely chiral nanoparticles or C-dots with chiral groups on the surface would form. Measurements of the circular dichroism signal showed that there is a low-intensity signal in the $300\text{--}500 \text{ nm}$ region. Its spectrum is presented in Fig. 4. In the spectral regions of $200\text{--}300$ and $500\text{--}800 \text{ nm}$, the signal-to-noise ratio was too low, indicating a lack of circular dichroism signal in these regions. It can be seen from Fig. 4 that in the $350\text{--}450 \text{ nm}$ region, which corresponds to the absorption of N, O-doped sp^2 domains of C-dots, a negative Cotton

effect is observed with a maximum at 386 nm, a minimum at 432 nm, and a circular dichroism value of +0.5 and –0.5 mdeg, respectively. Dissymmetry factor g was +0.8 and $-1.2 \cdot 10^{-5}$ for the positive and negative peaks, respectively. This value is 1–2 orders of magnitude smaller than the previously published values for C-dots obtained by the one-step method ($1.6 \cdot 10^{-3}$ [17] and $Fx43xE$ [22]). We predict that the presence of this signal is associated with the decomposition of glutathione molecules during solvothermal synthesis in the presence of formamide and the formation of N,O- doped sp^2 domains with a small number of chiral centers due to possible racemization at high synthesis temperatures. In most published studies into the synthesis of chiral C-dots, circular dichroism signals are observed in the region up to 350 nm and are mostly associated with the initial chiral precursor molecules or their aggregates covalently bound to the surface of C-dots [23–26]. The detection of circular dichroism signals due specifically to the internal structure of C-dots in the region above 350 nm is a rare observation and requires further research. It should also be noted that chiral C-dots synthesized in this work feature the longest-wavelength PL band known to date. In previous studies, the PL band was observed at 601 [24], 620 [25], and 630 nm [26] with quantum yields of 10.8, 6.8, and 16.2%, respectively.

Conclusion

In this work, chiral C-dots based on glutathione and formamide, which emit in the red region of the spectrum with a relatively high QY, were studied. The use of polymer in the synthesis did not affect the formation of optical centers of C-dots, but contributed to an increase in the size and number of aliphatic chains on the surface. C-dots possess their own chirality, which is caused by the formation of chiral centers inside N,O-doped aromatic domains when glutathione interacts with formamide. The nature of luminescence is associated with the formation of optical centers similar to macromolecules — derivatives of porphyrins embedded into the C-dot matrix. Thus, nanoparticles synthesized in this work are promising for further studies and application in biology and medicine as luminescent markers.

Acknowledgments

The authors express their gratitude to the center for collective use “Nanotechnology” of the ITMO University. Equipment provided by the resource center „Physical Methods of Surface Research“ at the Research Park of St. Petersburg University was used in XPS studies.

Funding

This study was supported by the Russian Science Foundation (grant № 22-13-00294).

Conflict of interest

The authors declare that they have no conflict of interest.

References

- [1] B. Wang, G.I.N. Waterhouse, S. Lu. *Trends Chem.*, **5** (1), 76 (2023). DOI: 10.1016/j.trechm.2022.10.005
- [2] E.A. Stepanidenko, E.V. Ushakova, A.V. Fedorov, A.L. Rogach. *Nanomaterials*, **11** (2), 364 (2021). DOI: 10.3390/nano11020364
- [3] R. Fu, H. Song, X. Liu, Y. Zhang, G. Xiao, B. Zou, G.I.N. Waterhouse, S. Lu. *Chinese J. Chem.*, **41** (9), 1007 (2023). DOI: 10.1002/CJOC.202200736
- [4] N. Gao, L. Huang, T. Li, J. Song, H. Hu, Y. Liu, S. Ramakrishna. *J. Appl. Polym. Sci.*, (2020). DOI: 10.1002/app.48443
- [5] A.A. Vedernikova, M.D. Miruschenko, I.A. Arefina, A.A. Babaev, E.A. Stepanidenko, S.A. Cherevkov, I.G. Spiridonov, D.V. Danilov, A.V. Koroleva, E.V. Zhizhin, E.V. Ushakova. *Nanomaterials*, **12** (19), 3314 (2022). DOI: 10.3390/NANO12193314/S1
- [6] M. Sbacchi, M. Mamone, L. Morbiato, P. Gobbo, G. Filippini, M. Prato. *ChemCatChem*, **15** (16), e202300667 (2023). DOI: 10.1002/CCTC.202300667
- [7] E. Liu, T. Liang, E.V. Ushakova, B. Wang, B. Zhang, H. Zhou, G. Xing, C. Wang, Z. Tang, S. Qu, A.L. Rogach. *J. Phys. Chem. Lett.*, **12** (1), 604 (2020). DOI: 10.1021/ACS.JPCLETT.0C03383
- [8] J. Wang, Y. Fu, Z. Gu, H. Pan, P. Zhou, Q. Gan, Y. Yuan, C. Liu. *Small*, (2023). DOI: 10.1002/smll.202303773
- [9] D. Li, E. V. Ushakova, A.L. Rogach, S. Qu. *Small*, **17** (43), 2102325 (2021). DOI: 10.1002/smll.202102325
- [10] E.A. Stepanidenko, I.D. Skurlov, P.D. Khavlyuk, D.A. Onishchuk, A.V. Koroleva, E.V. Zhizhin, I.A. Arefina, D.A. Kuryukov, D.A. Eurov, V.G. Golubev, A.V. Baranov, A.V. Fedorov, E.V. Ushakova, A.L. Rogach. *Nanomaterials*, **12** (3), (2022). DOI: 10.3390/nano12030543
- [11] D. Chen, M. Xu, W. Wu, S. Li. *J. Alloys Compd.*, **701**, 75 (2017). DOI: 10.1016/j.jallcom.2017.01.124
- [12] J. Zhu, X. Bai, J. Bai, G. Pan, Y. Zhu, Y. Zhai, H. Shao, X. Chen, B. Dong, H. Zhang, H. Song. *Nanotechnology*, **29** (8), 085705 (2018). DOI: 10.1088/1361-6528/aaa321
- [13] S. Sun, L. Zhang, K. Jiang, A. Wu, H. Lin. *Chem. Mater.*, **28** (23), 8659 (2016). DOI: 10.1021/acs.chemmater.6b03695
- [14] S. Zhou, Y. Sui, X. Zhu, X. Sun, S. Zhuo, H.Li. *Chem. — An Asian J.*, **16** (4), 348 (2021). DOI: 10.1002/asia.202001352
- [15] A. Dö ring, E. Ushakova, A.L. Rogach. *Light Sci. Appl.*, **11**, 75 (2022). DOI: 10.1038/s41377-022-00764-1
- [16] B. Bartolomei, A. Bogo, F. Amato, G. Ragazzon, M. Prato. *Angew. Chemie Int. Ed.*, **61** (20), e202200038 (2022). DOI: 10.1002/ANIE.202200038
- [17] A. Das, E. V. Kundelev, A.A. Vedernikova, S.A. Cherevkov, D. V. Danilov, A. V. Koroleva, E. V. Zhizhin, A.N. Tsyppin, A.P. Litvin, A. V. Baranov, A. V. Fedorov, E. V. Ushakova, A.L. Rogach. *Light Sci. Appl.*, **11**, 92 (2022). DOI: 10.1038/s41377-022-00778-9
- [18] A. Das, I.A. Arefina, D.V. Danilov, A.V. Koroleva, E. V. Zhizhin, P.S. Parfenov, V.A. Kuznetsova, A.O. Ismagilov,

- A.P. Litvin, A.V. Fedorov, E.V. Ushakova, A.L. Rogach. *Nanoscale*, **13** (17), (2021). DOI: 10.1039/d1nr01693h
- [19] J.R. Macairan, I. Zhang, A. Clermont-Paquette, R. Naccache, D. Maysinger. *Part. Part. Syst. Charact.*, **37** (1), (2020). DOI: 10.1002/ppsc.201900430
- [20] P. Gao, H. Hui, C. Guo, Y. Liu, Y. Su, X. Huang, K. Guo, W. Shang, J. Jiang, J. Tian. *Carbon NY.*, **201**, (2023). DOI: 10.1016/j.carbon.2022.09.052
- [21] Y. Ganjkhanlou, J.J.E. Maris, J. Koek, R. Riemersma, B.M. Weckhuysen, F. Meirer. *J. Phys. Chem. C*, **126** (5), (2022). DOI: 10.1021/acs.jpcc.1c10478
- [22] A. Visheratina, L. Hesami, A. K. Wilson, N. Baalbaki, N. Noginova, M. A. Noginov, N.A. Kotov. *Chirality*, **34** (12), (2022). DOI: 10.1002/chir.23509.
- [23] F. Li, Y. Li, X. Yang, X. Han, Y. Jiao, T. Wei, D. Yang, H. Xu, G. Nie. *Angewandte Chemie*, **130** (9), (2018). DOI: 10.1002/ange.201712453.
- [24] Y.Y. Wei, L. Chen, X. Zhang, J.L. Du, Q. Li, J. Luo, X.G. Liu, Y.Z. Yang, S.P. Yu, Y.D. Gao. *Biomater. Sci.*, **10** (15), (2022). DOI: 10.1039/d2bm00429a.
- [25] S. Wei, B. Wang, H. Zhang, C. Wang, S. Cui, X. Yin, C. Jiang, G. Sun. *Chem. Engineering J.*, **466**, (2023). DOI: 10.1016/j.cej.2023.143103.
- [26] Z. Hallaji, Z. Bagheri, B. Ranjbar. *ACS Appl Nano Mater*, **6** (5), (2023). DOI: 10.1021/acsnm.2c04466

Translated by D.Safin